Journal of Biomolecular NMR, 6 (1995) 171–179
ESCOM

J-Bio NMR 296

^{1}H, ^{13}C and ^{15}N NMR assignments and solution secondary structure of rat Apo-S100β

Judith C. Amburgey[a], Frits Abildgaard[c], Mary R. Starich[d], Sanjiv Shah[b,*], Dana C. Hilt[b,**] and David J. Weber[a,***]

Departments of [a]Biological Chemistry and [b]Neurology, University of Maryland School of Medicine, 108 North Greene Street, Baltimore, MD 21201, U.S.A.
[c]National Magnetic Resonance Facility at Madison, University of Wisconsin at Madison, 420 Henry Mall, Madison, WI 53706-1569, U.S.A.
[d]Howard Hughes Medical Institute and Department of Chemistry and Biochemistry, University of Maryland Baltimore County, Baltimore, MD 21228, U.S.A.

Received 4 May 1995
Accepted 2 June 1995

Keywords: S100β; Secondary structure; EF-hands; S100 proteins

Summary

The ^{1}H, ^{13}C and ^{15}N NMR assignments of the backbone and side-chain resonances of rat S100β were made at pH 6.5 and 37 °C using heteronuclear multidimensional NMR spectroscopy. Analysis of the NOE correlations, together with amide exchange rate and $^{1}H^{\alpha}$, $^{13}C^{\alpha}$ and $^{13}C^{\beta}$ chemical shift data, provided extensive secondary structural information. Thus, the secondary structure of S100β was determined to comprise four helices (Leu[3]-Ser[18], helix I; Lys[29]-Leu[40], helix II; Gln[50]-Glu[62], helix III; and Phe[70]-Ala[83], helix IV), four loops (Gly[19]-His[25], loop I; Ser[41]-Glu[49], loop II; Asp[63]-Gly[66], loop III; and Cys[84]-Glu[91], loop IV) and two β-strands (Lys[26]-Lys[28], β-strand I and Glu[67]-Asp[69], β-strand II). The β-strands were found to align in an antiparallel manner to form a very small β-sheet. This secondary structure is consistent with predictions that S100β contains two 'helix–loop–helix' Ca^{2+}-binding motifs known as EF-hands. The alignment of the β-sheet, which brings the two EF-hand domains of S100β into close proximity, is similar to that of several other Ca^{2+} ion-binding proteins.

Introduction

The S100 protein family is a highly conserved group of small acidic Ca^{2+}-binding proteins, initially discovered in the vertebrate nervous system (Moore, 1965; Kligman and Hilt, 1988; Donato, 1991; Hilt and Kligman, 1991). A principal member of the S100 family, S100β from brain tissue, contains 91 amino acids (10.5 kDa) and is highly conserved in a variety of mammalian species (Fig. 1). The gene for S100β is mapped to the Down's syndrome region (bands 21q22.2 and 22.3) of human chromosome 21 (Allore et al., 1988), and S100β levels are increased in regions of the brain near neuritic plaques for patients with Alzheimer's disease (Van Eldik and Griffin, 1994). S100β transgenic mice are found to undergo astrocytosis and neurite proliferation, suggesting that an excess of S100β may be relevant to the neuropathology observed for these cognitive diseases (Reeves et al., 1994).

Presumably, the biological functions of S100β and its corresponding disulfide-linked dimer, $(S100\beta)_2$, are related to the tightly regulated intra- and extracellular Ca^{2+} ion concentrations (Kligman and Marshak, 1985). Each S100β

*Present address: National Institutes of Health, Laboratory of Biochemical Genetics, NHLBI, Building 36, Room 4C12, 9000 Rockville Pike, Bethesda, MD 20892, U.S.A.
**Present address: AMGEN Inc., 1840 DeHavilland Drive, Thousand Oaks, CA 91320-1789, U.S.A.
***To whom correspondence should be addressed.

Supplementary Material: A table of the chemical shift values for the backbone and side-chain resonances of S100β has been deposited in the BioMagResBank chemical shift databank at the University of Wisconsin at Madison. The table of chemical shifts and six figures, illustrating the quality of data from the 3D HNCA, HN(CO)CA, HNCACB, CBCA(CO)NH, C(CO)NH, HOHAHA-HSQC, NOESY-HSQC, HMQC-NOESY-HMQC and 4D ^{13}C,^{15}N-edited NOESY experiments, are available as supplementary material from David J. Weber.

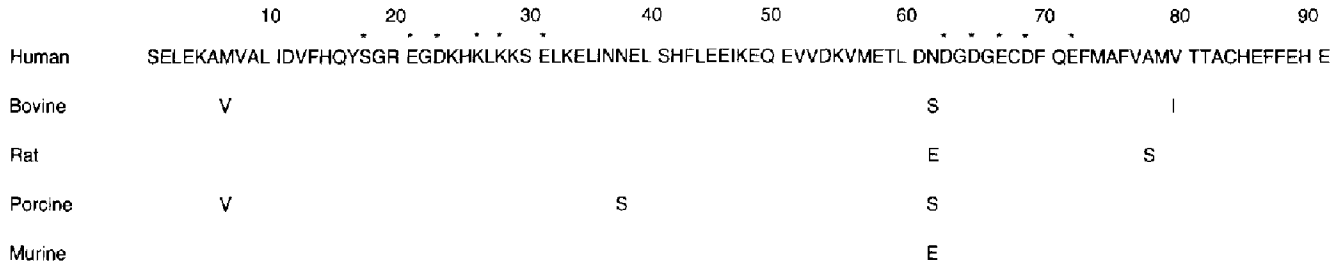

Fig. 1. Sequence homology of the S100β protein from several mammalian species. Only amino acids that differ from the human S100β sequence are shown. The amino acid residues proposed to form the putative Ca^{2+}-binding EF-hands are indicated by asterisks.

subunit has two classes of Ca^{2+}-binding sites, a high-affinity ($K_D = 20$ μM) and a significantly reduced binding affinity site ($K_D = 200$ μM) (Baudier et al., 1986; Kligman and Hilt, 1988). Thus, S100β is proposed to bind and modulate effector proteins in a manner similar to other Ca^{2+}-modulated proteins, such as calmodulin (Kligman and Hilt, 1988).

Based on sequence homologies to other Ca^{2+}-binding proteins (i.e., calmodulin, troponin C, etc.), S100β was predicted to contain two 'helix–loop–helix' Ca^{2+}-binding structural motifs known as EF-hands (Kretsinger, 1980; Kligman and Hilt, 1988; Strynadka and James, 1989). While the C-terminus of S100β contains 12 residues, typical of a normal EF-hand, the N-terminus contains an EF-hand with 14 residues that is referred to as a pseudo-EF-hand (ψ-EF-hand) (Strynadka and James, 1989; Skelton et al., 1994). Thus, rather than chelating Ca^{2+} with four side-chain carboxylate or carboxamide groups and a single backbone carbonyl oxygen, as done by typical EF-hands, the ψ-EF-hand in S100β is hypothesized to bind Ca^{2+} with four backbone carbonyls and a single side-chain carboxylate group in a manner analogous to the ψ-EF-hand present in another member of the S100 family, calbindin D_{9K} (Table 1) (Szebenyi and Moffat, 1986). To directly address the structural effects of Ca^{2+} binding to S100β, it is first necessary to examine S100β in the absence of Ca^{2+}. Thus, the structural determination of reduced apo-S100β in solution was initiated using heteronuclear multidimensional NMR spectroscopy techniques.

This study reports the ^1H, ^{13}C and ^{15}N resonance assignments and the secondary structure of reduced apo-S100β, determined by heteronuclear multidimensional NMR. The majority (98%) of the resonance assignments relied on triple-resonance experiments that provide sequential connectivities based on scalar coupling between ^{15}N- and ^{13}C-enriched nuclei (Bax and Grzesiek, 1993). Sequential NOE correlations were used to determine the remaining resonance assignments (2%) and to confirm the existing assignments as previously described (Wüthrich, 1986). The $^1H^\alpha$, $^{13}C^\alpha$ and $^{13}C^\beta$ secondary chemical shifts were also evaluated, in order to qualitatively analyze the secondary structure of S100β. The complete secondary structure determination relied on NOE correlations observed in 2D, 3D and 4D NMR spectra. Consistent with its stability, S100β was found to be a highly structured protein, even in the absence of metal ion. As a result of these studies, preliminary abstracts of this work have been published (Amburgey et al., 1994,1995). Ultimately, a direct structural comparison of apo-S100β, oxidized $(S100\beta)_2$ and their Ca^{2+} ion and Zn^{2+} ion complexes is planned.

Materials and Methods

Protein expression and purification

To permit higher expression yields in *Escherichia coli*, the rat S100β gene was cloned into an overexpression plasmid, pRE1 (Reddy et al., 1989), containing a λP_L promoter, and it was sequenced to verify the presence of the intact wild-type S100β gene (Kuwano et al., 1984; Maeda et al., 1991; Jiang et al., 1993; Shaw, S. and Hilt, D.C., unpublished data). Next, the S100β gene was subcloned into the *Nde*I and *Bam*HI restriction sites of the pET11b plasmid (Novagen, Inc., Madison, WI) under the control of a T7 promoter, as previously described (Abeygunawardana et al., 1993). The newly constructed plasmid was transformed into *E. coli* HB101 cells and sequenced

Abbreviations: CBCA(CO)NH, β- and α-carbon to nitrogen (via carbonyl) to amide proton correlation; C(CO)NH, side-chain carbon to nitrogen (via carbonyl) to amide proton correlation; DIPSI, decoupling in the presence of scalar interactions; DQF-COSY, double-quantum-filtered correlation spectroscopy; GARP, globally optimized alternating-phase rectangular pulses; HMQC, heteronuclear multiple-quantum coherence; HNCA, amide proton to nitrogen to α-carbon correlation; HNCACB, amide proton to nitrogen to α- and β-carbon correlation; HNCO, amide proton to nitrogen to carbonyl correlation; HN(CO)CA, amide proton to nitrogen to α-carbon (via carbonyl) correlation; HOHAHA, homonuclear Hartmann–Hahn spectroscopy; HSQC, heteronuclear single-quantum coherence; INEPT, insensitive nuclei enhancement by polarization transfer; βME, β-mercaptoethanol; MLEV, broadband decoupling pulse sequence developed by Malcolm Levitt; NOESY, nuclear Overhauser enhancement spectroscopy; ROESY, rotating frame Overhauser enhancement spectroscopy; SDS-PAGE, sodium dodecyl sulfate polyacrylamide gel electrophoresis; SLR, shaped radiofrequency pulse developed by Shinnar and LeRoux; Tris-HCl, tris(hydroxymethyl) amino-methane hydrochloride; TSP, sodium 3-(trimethylsilyl) propionate-2,2,3,3-d_4.

TABLE I
COMPARISON OF THE AMINO ACID SEQUENCES OF THE TWO PUTATIVE Ca^{2+}-BINDING SITES IN S100β WITH A CONSENSUS EF-HAND Ca^{2+}-BINDING SITE

	Position[a]											
	1	2	3	4	5	6	7	8	9	10	11	12
Consensus[b]	**D**	*B*	**D** **N**	G	**D** **N**	G	*X*	*H*	**O**	*H*	*A*	**E**
Ligand coordinate[c]	**X**		**Y**		**Z**		**–Y**		**–X**			**–Z**
S100β												
Site I[d] (ψ-EF-hand)	S	G R	E	G	D	K H	K	L	K	K	S	E
Site II[e] (normal EF-hand)	**D**	E	**D**	G	**D**	G	E	C	**D**	F	Q	**E**

[a] The position number is based on the consensus sequence for a normal EF-hand (Strynadka and James, 1989).
[b] Abbreviations include: *A*, acidic residue; *B*, basic residue; *H*, hydrophobic; *X*, any residue; *O*, Asp, Glu, Thr or Ser (Strynadka and James, 1989).
[c] The coordinates of the Ca^{2+} ligands are shown in bold, and the underlined coordinate has a carbonyl oxygen as the Ca^{2+} ligand, based on previously determined structures of EF-hand-containing proteins (Kretsinger, 1980).
[d] Underlined residues are proposed to have a carbonyl oxygen or H_2O (position 9) as the Ca^{2+} ligand, based on the three-dimensional structures of other pseudo-EF-hand-containing proteins (Szebenyi and Moffatt, 1986).
[e] The proposed Ca^{2+} ligands are shown in bold, and the underlined residue is proposed to have the carbonyl oxygen as the Ca^{2+} ligand, based on previously determined structures of EF-hand-containing proteins (Kretsinger, 1980).

again to verify the presence of the intact, wild-type S100β gene. The purified, S100β-containing plasmid was then transformed into *E. coli* strain HMS174 (DE3) cells (Novagen, Inc.), which grow well on media with minimal nutrients. S100β from the cell lysates was purified to >98% homogeneity at 4 °C under reducing conditions (1 mM βME), with some modifications of a previously reported procedure (Van Eldik et al., 1988)*. The processed S100β from the plasmid construction has an N-terminal methionine, as confirmed by N-terminal sequence analysis (data not shown). Purified recombinant protein with methionine as the first residue was previously shown to co-migrate on SDS-PAGE with S100β isolated from brain (which has serine as the first residue), react with S100β primary antibodies, dimerize in the presence of Ca^{2+}, and stimulate neurite outgrowth from cerebral cortex neurons with the same specific activity as the isolated brain S100β protein (Van Eldik et al., 1988; Amburgey et al., 1994; Drohat, A.C. and Weber, D.J., unpublished results). Thus, the additional N-terminal methionine has no known effect on reduced or oxidized S100β biological activities.

Complete amino acid analyses (Analytical Biotechnology Services, Boston, MA) confirmed the composition of our S100β preparations. These analyses also provided the protein concentration for two samples, and the extinction coefficient (ε) was then calculated from absorbance readings at 280 nm (A_{280}) to be 1986 ± 15 cm^{-1} for reduced S100β.

NMR sample preparation

NMR samples contained 3–6 mM S100β, 0.1 mM EDTA, 0.34 mM NaN_3, 2–10 mM βME, 6–10 mM d_{11}-Tris-HCl, and sufficient NaCl (17–20 mM) to give an ionic strength equal to 25 mM, unless otherwise stated. The pH was adjusted to a meter reading of 6.5 in H_2O (10% D_2O). All solutions were treated with Chelex-100 prior to their addition to the NMR sample. All NMR experiments were collected in 90% H_2O/10% D_2O at 37 °C. Uniformly ^{15}N-labeled NH_4Cl (99% ^{15}N) and ^{13}C-labeled glucose (>98% ^{13}C) were purchased from Cambridge Isotope Laboratories (Andover, MA) and deuterated d_{11}-Tris-HCl (1 M solution in D_2O, >99 atom percent deuterium) was purchased from C/D/N Isotopes, Inc. (Vandreuil, Quebec). D_2O (100.0 atom percent deuterium, low in paramagnetic impurities) was purchased from Aldrich Chemical Company (Milwaukee, WI). All other reagents for the NMR samples were of the highest purity commercially available.

NMR spectroscopy

A DQF-COSY (Piantini et al., 1982), a 2D clean-HOHAHA (Bax and Davis, 1985a) with a 70 ms spin-lock time, and a 2D NOESY (Jeener et al., 1979) with a mixing time of 200 ms were collected on a General Electrics OMEGA-PSG 600 NMR spectrometer (599.71 MHz, ^1H) fitted with a Bruker 5 mm triple-resonance probe. A 2D ROESY experiment (Bax and Davis, 1985b; Kessler et al., 1987) was recorded on a modified Bruker AM-600

*When compared to the elution of protein molecular weight standards (Pharmacia, Inc.) on a G100 gel filtration column, S100β eluted at a column volume equivalent to a protein with a molecular weight of 25.1 kDa, rather than at a volume typical for its molecular weight of 10.5 kDa. More accurate measurements of the molecular weight of reduced S100β are underway, and these results will be presented in a future publication. It should be noted, however, that the purified S100β is not the disulfide-linked dimer, $(S100\beta)_2$, based on SDS-PAGE using oxidized disulfide-linked dimer as a standard. Thus, if S100β is self-associating in reducing buffer, it is doing so via non-covalent binding.

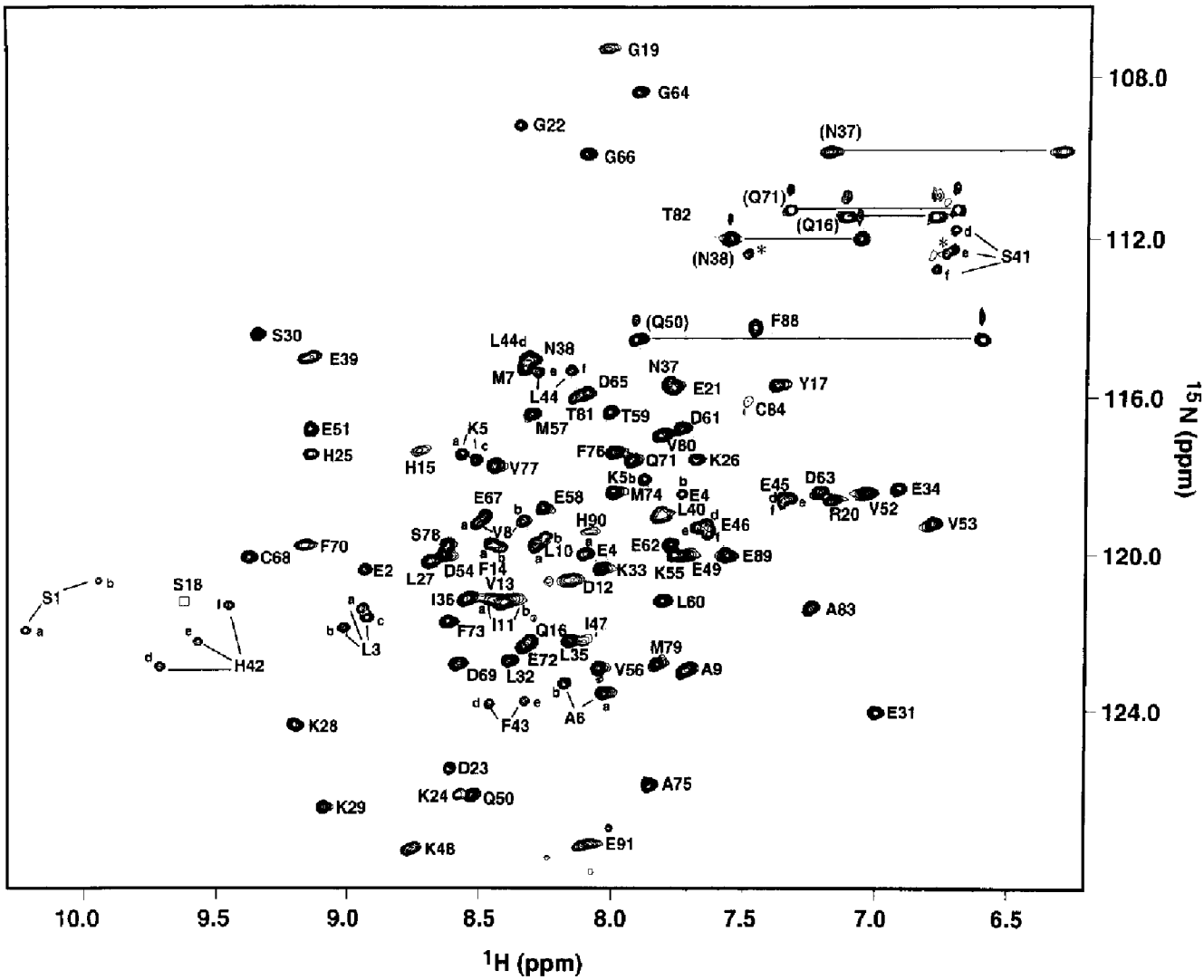

Fig. 2. Two-dimensional ^{1}H-^{15}N HSQC spectrum of reduced uniformly ^{15}N-labeled S100β at 600 MHz proton frequency. Correlation peaks are labeled according to residue type and sequence number. The correlations connected by horizontal lines correspond to glutamine and asparagine side-chain NH_2 groups. The assignments of the extra correlations for a single residue are labeled with the letters a–f. Multiple ^{1}H-^{15}N correlations for a single residue are grouped based on sequential NOE connectivities (i.e., 41d shows sequential NOE correlations with 42d, but not with 42e or 42f). Peaks labeled with an asterisk (*) were not observed in the triple-resonance NMR experiments. Conditions were: 6 mM uniformly ^{15}N-labeled S100β, 2 mM βME, 21 mM NaCl, 0.34 mM NaN_3, 0.1 mM EDTA, 5 mM d_{11}-Tris-HCl, pH 6.5, 37 °C.

spectrometer (600.13 MHz, ^{1}H) (Abeygunawardana et al., 1993) using a 90 ms spin-lock time.

Two-dimensional ^{1}H-^{15}N HSQC spectra (Bodenhausen and Ruben, 1980) were recorded as 256*×512* data matrices (* indicates complex data points) with acquisition times of 102.4 ms (^{15}N) and 143.4 ms (^{1}H). Hydrogen exchange of the amide protons was observed by lyophilizing S100β from H_2O and redissolving it in D_2O. Immediately following the addition of D_2O, a series of 2D ^{1}H-^{15}N HSQC spectra were collected at 0.25, 2.5, 8.5, 17.2, 20.8, 50.7, 54.3, 60.5 and 252 h, as described previously (Marion et al., 1989b). In a separate series of experiments, sensitivity-enhanced HSQC data (Palmer et al., 1991; Kay et al., 1992; Schleucher et al., 1994) were collected from 22 to 47 °C in 5° increments on a Bruker DMX 600 MHz NMR spectrometer.

Three-dimensional ^{15}N-edited NOESY-HSQC (Kay et al., 1989) spectra were collected using mixing times of 100 and 200 ms, and a 3D ^{15}N-edited clean-HOHAHA-HSQC (Bax and Davis, 1985a; Marion et al., 1989a) spectrum was recorded using a 70 ms MLEV-17 spin-lock period. For both experiments, presaturation of the H_2O and HDO resonances was achieved using phase-ramped SLR shaped pulses (Shinnar et al., 1989a,b). The final processed data matrices in these experiments contained 512×64×512 real points in the F1, F2 and F3 dimensions, respectively. A 3D ^{15}N,^{15}N-edited HMQC-NOESY-HMQC experiment (Ikura et al., 1990), using a 200 ms mixing time, was collected on a modified Bruker AM-600 (600.13 MHz, ^{1}H) spectrometer (Abeygunawardana et al., 1993), and the final processed data matrix consisted of 128×128×512 real points in the F1, F2 and F3 dimensions, respectively.

Heteronuclear HNCO (Kay et al., 1990; Grzesiek and Bax, 1992a), HNCA (Kay et al., 1990; Grzesiek and Bax, 1992a), HN(CO)CA (Bax and Ikura, 1991; Bax and Pochapsky, 1992; Grzesiek and Bax, 1992a), CBCA(CO)NH (Grzesiek and Bax, 1992b) and HNCACB (Wittekind and Mueller, 1993) experiments were recorded on a Bruker AM-500 (500.13 MHz, ^{1}H) spectrometer, modified as previously described (Mooberry et al., 1994). A C(CO)NH experiment (Grzesiek et al., 1993) was recorded on a Bruker DMX-600 (600.13 MHz, ^{1}H) spectrometer with a ^{13}C isotropic mixing time of 17.4 ms. The ^{15}N chemical shifts in all of these experiments were recorded in a constant-time manner (Powers et al., 1991), and z-axis pulsed field gradients were used to purge undesired transverse magnetization (Bax and Pochapsky, 1992). A sensitivity-enhanced 4D ^{13}C,^{15}N-edited NOESY experiment (Muhandiram et al., 1993) was recorded on a Bruker DMX-500 spectrometer using a 100 ms mixing time. The F4 dimension of the data was processed in the sensitivity-enhanced mode, as described previously (Palmer et al., 1991), and the final data matrix contained $64 \times 128 \times 32 \times 1024$ real points in the F1, F2, F3 and F4 dimensions, respectively.

The observed ^{1}H chemical shifts are reported with respect to the H_2O or HDO signal, which is taken as 4.658 ppm downfield from external TSP in D_2O (0.0 ppm) at 37 °C. The ^{15}N and ^{13}C chemical shift axes were indirectly referenced (Live et al., 1984; Spera and Bax, 1991; Edison et al., 1994) using the following ratios of the zero-point frequencies at 37 °C: 0.10132905 for ^{15}N to ^{1}H, and 0.25144953 for ^{13}C to ^{1}H.

Results

Sequential assignment of S100β

A resolution-enhanced ^{1}H-^{15}N HSQC spectrum of uniformly ^{15}N-labeled S100β shows correlation peaks for 88 of the 92 expected backbone amide resonances (Fig. 2). The four missing backbone $^1H^N$ and ^{15}N resonances correspond to Met^0, His^{85}, Glu^{86} and Phe^{87}, which remain unassigned. The spectrum shows 10 additional correlation peaks from the side-chain NH_2 groups of the two asparagine and three glutamine residues (peaks connected by horizontal lines in Fig. 2), and 22 additional correlation peaks from 14 residues giving multiple correlation peaks for a single residue in the ^{1}H-^{15}N HSQC spectrum (Ser^1, Leu^3, Glu^4, Lys^5, Ala^6, Val^8, Leu^{10}, Phe^{14}, Ser^{41}, His^{42}, Phe^{43}, Leu^{44}, Glu^{45} and Glu^{46}). In S100β, three residues (Met^7, Asn^{38} and Leu^{44}d) have overlapping ^{1}H-^{15}N correlations, and two other residues (Asp^{54} and Ser^{78}) are barely resolved based on the digital resolution of the HSQC spectrum (^{1}H, 0.01 ppm/point; ^{15}N, 0.08 ppm/point). Initial attempts to make sequential assignments for S100β using 2D homonuclear NMR data (NOESY, DQF-COSY, HOHAHA, ROESY) were unsuccessful, due to chemical shift degeneracies. Specifically, 59 of the 90 assigned H^α resonances appear within 1.0 ppm (3.80–4.80 ppm) and 57 of the 88 assigned H^N resonances appear within a 1.0 ppm window (7.60–8.60 ppm). Thus, 3D data from the HNCA, HN(CO)CA, HNCACB, CBCA(CO)NH and C(CO)NH triple-resonance experiments were necessary to unambiguously complete the sequential resonance assignments of S100β. Note that there was no need for H_2O-D_2O corrections in any of the reported chemical shifts, because all of the S100β NMR experiments were conducted in H_2O.

The occurrence of multiple ^{1}H-^{15}N correlations for a single residue can explain why more than the expected 92 ^{1}H-^{15}N backbone correlations are observed in the HSQC spectrum of S100β. The first convincing evidence for multiple ^{1}H-^{15}N correlations for a single residue was found for residue Lys^5. Here, the side-chain resonances observed in the 3D ^{15}N-edited HOHAHA-HSQC spectrum were the same as two previously unassigned ^{1}H-^{15}N correlation peaks. Furthermore, the chemical shift values for the $^{13}C_i^\alpha$, $^{13}C_{i-1}^\alpha$, $^{13}C_i^\beta$, $^{13}C_{i-1}^\beta$, and preceding side-chain ^{13}C resonances were found to be the same for each of the three respective ^{1}H to ^{15}N correlations assigned to residue Lys^5. Once the possibility of multiple ^{1}H-^{15}N correlations for a single residue was recognized, the identification and assignment of the other residues of S100β with multiple ^{1}H-^{15}N correlations followed in the same manner.

The sequential assignment process began by identifying the four glycine and four alanine residues of S100β, based on their characteristic $^{13}C^\alpha$ (≈ 45 ppm) and $^{13}C^\beta$ (≈ 17 ppm) chemical shift values, respectively (Grzesiek and Bax, 1993), and on their amino acid-type assignments from the 3D ^{15}N-edited HOHAHA-HSQC spectrum. Thus, Ala^6-Ala^9, Gly^{19}-Gly^{22}, Gly^{64}-Gly^{66}, Ala^{75} and Thr^{82}-Ala^{83} were used as starting points in the sequential assignment procedure. Next, stretches of amino acids were aligned sequentially by matching the $^{13}C_{i-1}^\alpha$ and $^{13}C_{i-1}^\beta$ interresidue chemical shifts of one residue with the $^{13}C_i^\alpha$ and $^{13}C_i^\beta$ intraresidue chemical shifts of the neighboring residue, using data from the HNCA, HN(CO)CA, HNCACB, and CBCA(CO)NH experiments. The C(CO)NH experiment confirmed the $^{13}C^\alpha$,$^{13}C^\beta$ chemical shift data from the HNCA, HN(CO)CA, HNCACB and CBCA(CO)NH experiments, and it provided assignments for the remaining side-chain carbons. Additionally, short-range H^NH^N(i,i+1), $H^\alpha H^N$(i,i+1), $H^\beta H^N$(i,i+1), and medium-range H^NH^N(i,i+2), $H^\alpha H^N$(i,i+2), $H^\alpha H^N$(i,i+3) and $H^\alpha H^N$(i,i+4) NOE correlations observed in the 3D ^{15}N-edited NOESY-HSQC, 3D ^{15}N,^{15}N-edited HMQC-NOESY-HMQC, and 4D ^{13}C,^{15}N-edited NOESY spectra confirmed all of the sequential resonance assignments.

Secondary structure determination

The secondary structure of S100β was determined based on resonance assignments, chemical shift values

Fig. 3. Diagram of amide exchange, NOE connectivities, sequential connectivities and the secondary structure determined for reduced S100β. Circles indicate relative amide hydrogen exchange rates at 37 °C as determined using 2D ^{1}H-^{15}N HSQC spectra, described in Materials and Methods. Residues with no symbol ($T \leq 0.25$ h) are arbitrarily referred to as fast exchanging amide protons. Residues with half-shaded circles ($0.25\ h < T < 17.2$ h) are arbitrarily referred to as medium exchanging amide protons. Residues with solid circles ($T \geq 17.2$ h) are arbitrarily referred to as slowly exchanging amide protons. The NOE correlations were determined from 3D ^{15}N-edited NOESY-HSQC, 3D ^{15}N,^{15}N-edited HMQC-NOESY-HMQC and 4D ^{13}C,^{15}N-edited NOESY experiments at 37 °C as described in Materials and Methods. The height of the bar indicates the strength of the NOE (strong, medium, weak or very weak) and a dashed bar indicates that the NOE is tentatively assigned, due to overlap in chemical shift. Deviations in the $^{13}C^{\alpha}$ and $^{1}H^{\alpha}$ chemical shift from those of a random coil are illustrated such that regions of contiguous upfield-shifted $^{13}C^{\alpha}$ chemical shifts (positive values) and downfield-shifted $^{1}H^{\alpha}$ chemical shifts (negative values) are indicative of helical regions. Likewise, regions of contiguous downfield-shifted $^{13}C^{\alpha}$ chemical shifts (negative values) and upfield-shifted $^{1}H^{\alpha}$ chemical shifts (positive values) are indicative of regions of β-sheet (Spera and Bax, 1991; Wishart et al., 1991,1992; Wishart and Sykes, 1994). The secondary shifts for $^{13}C^{\beta}$ (data not shown) are consistent with the secondary structure derived from the NOE correlations. Secondary structure is represented by α-helices (spirals), β-strands (arrows) and loops (no symbol), as indicated under the appropriate residues in the sequence of reduced S100β.

(Spera and Bax, 1991; Wishart et al., 1991,1992; Wishart and Sykes, 1994), NOE data (Wüthrich, 1986) and amide exchange rate data (Wüthrich, 1986) (Fig. 3). These results indicate that S100β has four helices (60% helical content), separated by four loops (28% total random content) and a small two-stranded antiparallel β-sheet (6% β-strand content). This secondary structure is consistent with predictions both from CD spectroscopy (55–58% helical content) (Mani et al., 1982,1983) and from sequence homologies that S100β contains two EF-hand Ca^{2+}-binding motifs (Hilt and Kligman, 1991).

Helices

The four helices (I, Leu^{3}-Ser^{18}; II, Lys^{29}-Leu^{40}; III, Gln^{50}-Glu^{62}; IV, Phe^{70}-Ala^{83}) contain characteristic stretches of $H^{N}H^{N}(i,i+1)$ and weaker $H^{\alpha}H^{N}(i,i+1)$ NOE correlations (Fig. 3). Furthermore, each helix has $H^{\beta}H^{N}(i,i+1)$, $H^{\alpha}H^{N}$-$(i,i+3)$ and $H^{\alpha}H^{N}(i,i+4)$ NOE correlations that are typical for an α-helix (Wüthrich, 1986). The presence of weak noncontiguous $H^{\alpha}H^{N}(i,i+2)$ NOE correlations can probably be explained by spin diffusion; however, it is difficult to rule out the presence of some 3_{10}-helix character (i.e., especially in helix IV). Also, downfield-shifted $^{13}C^{\alpha}$ and upfield-shifted $^{1}H^{\alpha}$ resonances are observed in all helical residues, as expected (Fig. 3) (Spera and Bax, 1991; Wishart et al., 1992). The relatively small upfield secondary shift for the $^{13}C^{\alpha}$ resonance of residue His^{15} in helix I is probably due to the ionization state of the imidazole ring (Spera and Bax, 1991). Additionally, several amide protons of each helix have exchange rates of ≥ 17.2 h (Fig. 3), which is indicative of the hydrogen-bond network expected for helices.

β-sheet and loops

The predicted Ca^{2+}-binding domains, I (Ser^{18}-Glu^{31}) and II (Asp^{61}-Glu^{72}) (Table 1) (Kligman and Hilt, 1988), each contain a short β-strand segment, Lys^{26}-Leu^{27}-Lys^{28} (β-strand I) and Glu^{67}-Cys^{68}-Asp^{69} (β-strand II), respectively.

This observation is based on strong $H^{\alpha}H^{N}(i,i+1)$ NOE connectivities, as well as on upfield-shifted $^{13}C^{\alpha}$ and downfield-shifted $^{13}C^{\beta}$ and $^{1}H^{\alpha}$ resonances that are characteristic of β-strand secondary structure (Wüthrich, 1986; Spera and Bax, 1991; Wishart et al., 1992) (Fig. 3). The presence of unambiguous long-range NOE correlations between the two β-strands, observed in the 2D NOESY, 3D ^{15}N-edited NOESY-HSQC, 3D ^{15}N,^{15}N-edited HMQC-NOESY-HMQC, and 4D ^{13}C,^{15}N-edited NOESY spectra, is consistent with these strands aligning in an antiparallel fashion (Fig. 4). Additionally, residues in the β-sheet are marked by a number of slowly exchanging amide protons, indicative of hydrogen bonding or solvent inaccessibility.

The remaining residues of S100β are found in four loops (I, Gly^{19}-His^{25}; II, Ser^{41}-Glu^{49}; III, Asp^{63}-Gly^{66}; and IV, Cys^{84}-Glu^{91}). Residues His^{85} through Phe^{87} in loop IV are proposed to be involved in slow conformational averaging, due to the absence of their ^{1}H-^{15}N correlations in the NMR spectra.

Discussion

The ^{1}H, ^{15}N and ^{13}C backbone and side-chain resonances of rat apo-S100β were nearly completely assigned by a combination of 2D, 3D and 4D heteronuclear NMR methods at pH 6.5 and 37 °C. These resonance assignments were used to interpret the short- and medium-range interproton NOE correlations necessary for the elucidation of the solution secondary structure of S100β. The ^{1}H, $^{13}C^{\alpha}$ and $^{13}C^{\beta}$ secondary chemical shifts were consistent with the secondary structure determined from the NOE correlations. The secondary structure of S100β was found to consist of four helices, four loops and two β-strands.

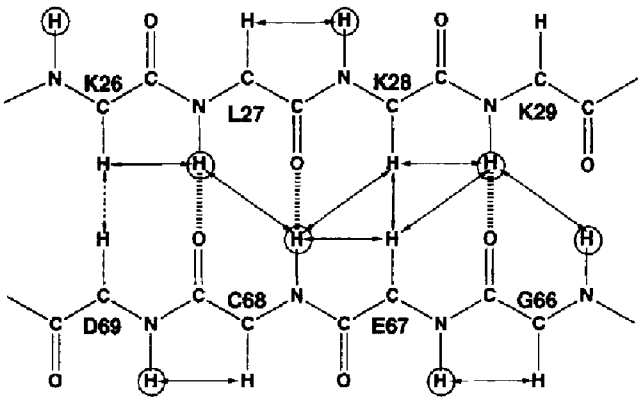

Fig. 4. Diagram of the two antiparallel β-strands present in reduced S100β. Solid arrows indicate the sequential $H^{N}H^{N}(i,i+1)$ and $H^{\alpha}H^{N}(i,i+1)$ and the long-range $H^{N}H^{N}(i,j)$, $H^{\alpha}H^{N}(i,j)$ and $H^{\alpha}H^{\alpha}(i,j)$ NOE correlations observed in the 2D NOESY, 3D ^{15}N-edited NOESY-HSQC, 3D ^{15}N,^{15}N-edited HMQC-NOESY-HMQC and/or 4D ^{13}C, ^{15}N-edited NOESY spectra. The dashed arrow represents an NOE correlation that is tentatively assigned, due to chemical shift overlap. Hashed lines represent hydrogen bonds, derived from slow amide hydrogen exchange (circled protons), and the structure of the β-sheet, derived from the long-range NOE correlations observed.

The β-strands align in an antiparallel fashion to form a small β-sheet that brings the two Ca^{2+}-binding domains of S100β into close proximity.

An intriguing observation made during the sequential assignment and secondary structure determination of S100β is that two regions of the protein (helix I and loop II) exhibit two or three ^{1}H-^{15}N correlations for a single amino acid residue. Multiple resonances can be attributed to inhomogeneous samples (Driscoll et al., 1990; Forman-Kay et al., 1990) or to nuclei coexisting as two (or more) subspecies in equilibrium. In the latter case, multiple correlations arise because the interconversion between the various states is relatively slow on the chemical shift time scale (Bovey et al., 1988). Two causes of multiple correlations in a homogeneous protein sample are proline isomerization (Chazin et al., 1989; Kördel et al., 1990) or disulfide bond isomerization (Pallaghy et al., 1993). For S100β, the lack of proline residues or disulfides quickly eliminates these explanations for the multiple peaks observed. In addition, these processes can only provide explanations for peak doubling, whereas we observe three correlations for a single residue in several cases. It is also clear that the nuclei displaying multiple resonances are not interchanging between conformational states, because a majority of these resonances (≈ 70%) exhibit a narrowing of ^{1}H and ^{15}N line widths as the temperature is increased from 22 to 47 °C in HSQC experiments (data not shown). Thus, for this temperature range, S100β probably exists as three independent subspecies, with energy barriers between these states sufficiently high to prevent their interconversion on the NMR time scale.

The homogeneity (>98%) of our S100β preparations was determined by amino acid analysis, N-terminal protein sequencing and SDS-PAGE, which rule out an impure sample as the cause of multiple correlations for a single residue. Furthermore, subsequent oxidation of cysteine residues is unlikely, because β-mercaptoethanol was present in all buffers during the protein preparation and in the final NMR sample. Moreover, the NMR samples were stored under argon in sealed NMR tubes. The relative intensity of the multiple correlations did not show any change over time (> 1 year), suggesting that oxidation did not occur during the course of the NMR experiments. Finally, several preparations of S100β gave identical NMR spectra, with the multiple peaks having the same relative intensity. This further indicates that various oxidation states and/or inhomogeneous S100β samples were not used in these studies.

The secondary structure determined is consistent with predictions that a pseudo-EF-hand (ψ-EF-hand) is present at the N-terminus and a classical EF-hand is present at the C-terminus of S100β. The ψ-EF-hand comprises residues from helix I, loop I, β-strand I and helix II, and the classical EF-hand comprises residues from helix III, loop III, β-strand II and helix IV. Residues of each Ca^{2+}-

binding domain are positioned relative to the consensus sequence of the classical EF-hand in Table 1, and Ca^{2+} ligands for the ψ-EF-hand are based on the structure of calbindin D_{9K}, another member of the S100 family of proteins (Szebenyi and Moffat, 1986). Like S100β, calbindin D_{9K} contains four helices and a small antiparallel β-sheet. In both proteins, the antiparallel β-sheet brings the ψ-EF-hand and the classical EF-hand together (Szebenyi and Moffat, 1986; Skelton et al., 1990a,b; Akke et al., 1992; Kördel et al., 1993). Similarly, a small antiparallel β-sheet is also observed between EF-hand domains in several other proteins of the calmodulin superfamily (Strynadka and James, 1989).

The region of S100β with the least sequence homology to other S100-family proteins is loop II, and thus this is referred to as the 'hinge' region in S100 proteins (Kligman and Hilt, 1988). Interestingly, the analogous 'hinge' region in calbindin D_{9K} (residues 41–44) was found to be mobile, as judged by low order parameters calculated from NMR relaxation rate data (Kördel et al., 1992,1993) and high B factors in the crystal structure (Szebenyi and Moffat, 1986). A peptide corresponding to the 'hinge' region in another S100 protein, CP-10, was synthesized. Interestingly, this synthetic peptide exhibited the same chemotactic activity as that of the corresponding full-length protein (Lackmann et al., 1993). It was concluded that the 'hinge' region of CP-10 contributed significantly to the protein's functional specificity, but sustained activity was found to be dependent on the structural integrity of the entire protein. Thus, in a manner similar to CP-10, loop II of S100β may be responsible for the functional specificity of the protein. Interestingly, this loop exhibits multiple ^{1}H-^{15}N correlations, indicative of it being in multiple magnetic environments in reduced apo-S100β.

Conclusions

The NMR assignments and secondary structure provide the basis for elucidation of the complete three-dimensional solution structure of reduced apo-S100β. This study also provides a starting point for the sequential assignment and structural determination processes for both the Ca^{2+} and Zn(II) complexes of S100β. A comparison of these structures will give insight into the functional role of the 'hinge' region of S100β and the complex relationship between its various metal ion complexes and dimerization states necessary for biological function.

Acknowledgements

We are grateful to Dr. Mike Summers and Dr. Clemens Anklin for NMR instrument time, and to Alex Drohat, Dr. Chitrananda Abeygunawardana, and the reviewers of this paper for their very helpful suggestions in the preparation of the manuscript. We are also grateful to Clara Mortezai-Zanjani at the BioMagResBank for assistance with the chemical shift database. This study made use of the National Magnetic Resonance Facility at Madison, which is supported by NIH Grant RR02301 from the Biomedical Research Technology Program, National Center for Research Resources. Equipment in the facility was purchased with funds from the University of Wisconsin, the NFS Biological Instrumentation Program (Grant DMB-8415048), the NIH Biomedical Research Technology Program (Grant RR02301), the NIH Shared Instrumentation Program (Grant RR02781) and the U.S. Department of Agriculture. This work is supported by Grant R29GM52071-01 from the NIH (to D.J.W.) and by SRIS and DRIF funding from the State of Maryland.

References

Abeygunawardana, C., Weber, D.J., Frick, D.N., Bessman, M.J. and Mildvan, A.S. (1993) *Biochemistry*, **32**, 13071–13080.

Akke, M., Drakenberg, T. and Chazin, W.J. (1992) *Biochemistry*, **31**, 1011–1020.

Allore, R., O'Hanlon, D., Price, R., Neilson, K., Willard, H.F., Cox, D.R., Marks, A. and Dunn, R.J. (1988) *Science*, **239**, 1311–1313.

Amburgey, J.C., Abildgaard, F., Starich, M.R., Shah, S., Hilt, D.C. and Weber, D.J. (1994) *Abstracts of the 208th National ACS Meeting*, Biological Division, Poster 48, Washington, DC.

Amburgey, J.C., Abildgaard, F., Starich, M.R., Shah, S., Hilt, D.C. and Weber, D.J. (1995) *FASEB J.*, **9**, 1008.

Baudier, J., Glasser, N. and Gérard, D. (1986) *J. Biol. Chem.*, **261**, 8192–8203.

Bax, A. and Davis, D. (1985a) *J. Magn. Reson.*, **65**, 355–360.

Bax, A. and Davis, D. (1985b) *J. Magn. Reson.*, **63**, 207–213.

Bax, A. and Ikura, M. (1991) *J. Biomol. NMR*, **1**, 99–104.

Bax, A. and Pochapsky, S. (1992) *J. Magn. Reson.*, **99**, 638–643.

Bax, A. and Grzesiek, S. (1993) In *NMR of Proteins* (Eds, Clore, G.M. and Gronenborn, A.M.), CRC Press, Boca Raton, FL, pp. 33–52.

Bodenhausen, G. and Ruben, D.J. (1980) *Chem. Phys. Lett.*, **69**, 185–188.

Bovey, F.A., Jelinski, L. and Mirau, P.A. (1988) *Nuclear Magnetic Resonance Spectroscopy*, 2nd ed., Academic Press, San Diego, CA.

Chazin, W.J., Kördel, J., Drakenberg, T., Thulin, E., Brodin, P., Grundström, T. and Forsén, S. (1989) *Proc. Natl. Acad. Sci. USA*, **86**, 2195–2198.

Donato, R. (1991) *Cell Calcium*, **12**, 713–726.

Driscoll, P.C., Clore, G.M., Marion, D., Wingfield, P.T. and Gronenborn, A.M. (1990) *Biochemistry*, **29**, 3542–3556.

Edison, A.S., Abildgaard, F., Westler, W.M., Mooberry, E.S. and Markley, J.L. (1994) *Methods Enzymol.*, **239**, 3–79.

Forman-Kay, J.D., Gronenborn, A.M., Kay, L.E., Wingfield, P.T. and Clore, M. (1990) *Biochemistry*, **29**, 1566–1572.

Grzesiek, S. and Bax, A. (1992a) *J. Magn. Reson.*, **96**, 432–450.

Grzesiek, S. and Bax., A. (1992b) *J. Am. Chem. Soc.*, **114**, 6291–6293.

Grzesiek, S., Anglister, J. and Bax, A. (1993) *J. Magn. Reson. Ser. B*, **101**, 114–119.

Grzesiek, S. and Bax, A. (1993) *J. Biomol. NMR*, **3**, 185–204.

Hilt, D.C. and Kligman, D. (1991) In *Novel Calcium-Binding Proteins* (Ed., Heizmann, C.), Springer, Berlin.

Ikura, M., Bax, A., Clore, G.M. and Gronenborn, A.M. (1990) *J. Am. Chem. Soc.*, **112**, 9020–9022.

Jeener, J., Meier, B.H., Bachmann, P. and Ernst, R.R. (1979) *J. Chem. Phys.*, **71**, 4546–4553.

Jiang, H., Shah, S. and Hilt, D.C. (1993) *J. Biol. Chem.*, **268**, 20502–20511.

Kay, L.E., Marion, D. and Bax, A. (1989) *J. Magn. Reson.*, **84**, 72–84.

Kay, L.E., Ikura, M., Tschudin, R. and Bax, A. (1990) *J. Magn. Reson.*, **89**, 496–514.

Kay, L.E., Keifer, P. and Saarinen, T. (1992) *J. Am. Chem. Soc.*, **114**, 10663–10665.

Kessler, H., Griesinger, C., Kerssebaum, R., Wagner, K. and Ernst, R.R. (1987) *J. Am. Chem. Soc.*, **109**, 607–609.

Kligman, D. and Marshak, D.R. (1985) *Proc. Natl. Acad. Sci. USA*, **82**, 7136–7139.

Kligman, D. and Hilt, D.C. (1988) *Trends Biochem. Sci.*, **13**, 437–443.

Kördel, J., Forsén, S., Drakenberg, T. and Chazin, W.J. (1990) *Biochemistry*, **29**, 4400–4409.

Kördel, J., Skelton, N.J., Akke, M., Palmer, A.G. and Chazin, W.J. (1992) *Biochemistry*, **31**, 4856–4866.

Kördel, J., Skelton, N.J., Akke, M. and Chazin, W.J. (1993) *J. Mol. Biol.*, **231**, 711–734.

Kretsinger, R.H. (1980) *CRC Crit. Rev. Biochem.*, **8**, 119–174.

Kuwano, R., Usui, H., Maeda, T., Fukui, T., Yamanari, N., Ohtsuka, E., Ikehara, M. and Takahashi, Y. (1984) *Nucleic Acids Res.*, **12**, 7455–7465.

Lackmann, M., Rajasekariah, P., Iismaa, S.E., Jones, G., Cornish, C.J., Hu, S., Simpson, R.J., Moritz, R.L. and Geczy, C.L. (1993) *J. Immunol.*, **150**, 2981–2991.

Live, D.H., Davis, D.G., Agosta, W.C. and Cowburn, D. (1984) *J. Am. Chem. Soc.*, **106**, 1939–1941.

Maeda, T., Usui, H., Araki, K., Kuwano, R., Takahashi, Y. and Suzuki, Y. (1991) *Mol. Brain Res.*, **10**, 193–202.

Mani, R.S., Boyes, B.E. and Kay, C.M. (1982) *Biochemistry*, **21**, 2607–2612.

Mani, R.S., Shelling, J.G., Sykes, B.D. and Kay, C.M. (1983) *Biochemistry*, **22**, 1734–1740.

Marion, D., Driscoll, P.C., Kay, L.E., Wingfield, P.T., Bax, A., Gronenborn, A.M. and Clore, G.M. (1989a) *Biochemistry*, **28**, 6150–6156.

Marion, D., Ikura, M., Tschudin, R. and Bax, A. (1989b) *J. Magn. Reson.*, **85**, 393–399.

Mooberry, E.S., Abildgaard, F. and Markley, J.L. (1994) *Methods Enzymol.*, **239**, 247–256.

Moore, B.E. (1965) *Biochem. Biophys. Res. Commun.*, **19**, 739–744.

Muhandiram, D.R., Guang, Y.X. and Kay, L.E. (1993) *J. Biomol. NMR*, **3**, 463–470.

Pallaghy, P.K., Duggan, B.M., Pennington, M.W. and Norton, R.S. (1993) *J. Mol. Biol.*, **234**, 405–420.

Palmer, A.G., Cavanagh, J., Wright, P.E. and Rance, M. (1991) *J. Magn. Reson.*, **93**, 151–170.

Piantini, U., Sørensen, O.W. and Ernst, R.R. (1982) *J. Am. Chem. Soc.*, **104**, 6800–6801.

Powers, R., Gronenborn, A.M., Clore, G.M. and Bax, A. (1991) *J. Magn. Reson.*, **94**, 209–213.

Reddy, P., Peterkofsky, A. and McKenney, K. (1989) *Nucleic Acids Res.*, **17**, 10473–10488.

Reeves, R.H., Yao, J., Crowley, M.R., Buck, S., Zhang, X., Yarowsky, P., Gearhart, J.D. and Hilt, D.C. (1994) *Proc. Natl. Acad. Sci. USA*, **91**, 5359–5363.

Schleucher, J., Schwendinger, M., Sattler, M., Schmidt, O., Schedletzky, S.J., Sørensen, O.W. and Griesinger, C. (1994) *J. Biomol. NMR*, **4**, 301–306.

Shinnar, M., Bolinger, L. and Leigh, J.S. (1989a) *Magn. Reson. Med.*, **12**, 88–92.

Shinnar, M., Eleff, S., Subramanian, H. and Leigh, J.S. (1989b) *Magn. Reson. Med.*, **12**, 74–80.

Skelton, N.J., Forsén, S. and Chazin, W.J. (1990a) *Biochemistry*, **29**, 5752–5761.

Skelton, N.J., Kördel, J., Forsén, S. and Chazin, W.J. (1990b) *J. Mol. Biol.*, **213**, 593–598.

Skelton, N.J., Kördel, J., Akke, M., Forsén, S. and Chazin, W.J. (1994) *Nature Struct. Biol.*, **1**, 239–245.

Spera, S. and Bax, A. (1991) *J. Am. Chem. Soc.*, **113**, 5490–5492.

Strynadka, N.C.J. and James, M.N.G. (1989) *Annu. Rev. Biochem.*, **58**, 951–998.

Szebenyi, D.M.E. and Moffat, K. (1986) *J. Biol. Chem.*, **261**, 8761–8777.

Van Eldik, L.J., Staecker, J.L. and Winningham-Major, F. (1988) *J. Biol. Chem.*, **263**, 7830–7837.

Van Eldik, L.J. and Griffin, W.S.T. (1994) *Biochim. Biophys. Acta*, **1223**, 398–403.

Wishart, D.S., Sykes, B.D. and Richards, F.M. (1991) *J. Mol. Biol.*, **222**, 311–333.

Wishart, D.S., Sykes, B.D. and Richards, F.M. (1992) *Biochemistry*, **31**, 1647–1651.

Wishart, D.S. and Sykes, B.D. (1994) *J. Biomol. NMR*, **4**, 171–180.

Wittekind, M. and Mueller, L. (1993) *J. Magn. Reson. Ser. B*, **101**, 201–205.

Wüthrich, K. (1986) *NMR of Proteins and Nucleic Acids*, Wiley, New York, NY.